DØ Note 5067-CONF

Search for Fermiophobic Higgs Boson in $3\gamma+X$ Events

The DØ Collaboration
URL http://www-d0.fnal.gov
(Dated: January 04, 2007)

Abstract

We report the results of a search for an excess of $3\gamma+X$ events in 0.83 ± 0.05 fb^{-1} of data collected by the DØ experiment at the Tevatron during the period 2002-2005. We estimate the backgrounds that are dominated by Direct Triphoton Production(DTP) and observe no excess of events above the Standard Model prediction. Thus, we set constraints on production rates of a fermiophobic Higgs boson in Two Higgs Doublet and Triplet Higgs Models.

Preliminary Results for Winter 2007 Conferences

1 Theoretical Motivation

The Standard Model describes our world at current experimentally accessible energies. However, the exact mechanism for EWSB remains a mystery. The spontaneous symmetry breaking mechanism requires a single doublet of complex scalar fields. But does Nature follow this minimalistic version or does it require a multi-Higgs sector or something completely different?

In a more general framework where the parameter content of the theory is richer, we may expect deviations from the SM predictions in the form of significant changes in the Higgs boson discovery signatures. One such example is the so-called "fermiophobic" Higgs boson, which has suppressed couplings to all fermions. It may arise in a variety of models (e.g. [1]). A variation of this theme is the Higgs boson in certain top-color models, which may couple only to heavy quarks [2]. Some even more exotic possibilities have been suggested in the context of theories with large extra dimensions [3]. Finally, in the Minimal Supersymmetric Standard Model (MSSM), the width into $b\bar{b}$ pairs can be suppressed due to 1-loop supersymmetry (SUSY) corrections, thus enhancing the branching ratios of a light Higgs boson into more exotic signatures [4, 5]. In all these cases, for masses $m_h < 100$ GeV/c^2 the Higgs boson decays to photon pairs [6]. Decays are mediated through a W or a heavy quark loop.

Experimental searches for fermiophobic higgs (h_f) at LEP and the Tevatron have yielded negative results. Mass limits have been set in a benchmark model that assumes that coupling h_fVV ($V \equiv W^{\pm}, Z$) has the same strength as in the Standard Model and that all fermion Branching Ratios (BR) are exactly zero. Combination of results obtained by the LEP collaborations OPAL [7], DELPHI [8], ALEPH [9], and L3 [10] yielded lower bound $m_h > 108.3$ GeV/c^2. This result was obtained utilizing channel $e^+e^- \to h_fZ,\ h_f \to \gamma\gamma$. In Run 1 of the Tevatron, the limits on m_{h_f} from the DØ and CDF collaborations are respectively 78.5 GeV/c^2 [11] and 82 GeV/c^2 [12] at 95% C.L., using the mechanism $qq' \to V^*h_fV,\ h_f \to \gamma\gamma$, with the dominant contribution coming from $V = W^{\pm}$. A preliminary search in the inclusive $2\gamma + X$ channel has been performed with 190 pb^{-1} of Run 2a data [15]. For an integrated luminosity of 2 fb^{-1}, Run 2 will extend the coverage of m_{h_f} in the benchmark model slightly beyond that of LEP [13, 14]. In addition, Run 2 will be sensitive to the region $110 < m_{h_f} < 160$ GeV/c^2 and BR($h_f \to \gamma\gamma$) > 4% which could not be probed at LEP.

However, the h_fVV coupling in a specific model could be suppressed relative to the $h_{SM}VV$ coupling by a mixing angle[1], leading to a weakening of the above mass limits. If this suppression were quite severe ($h_fVV/h_{SM}VV < 0.1$), a very light h_f ($m_{h_f} \ll 100$ GeV/c^2) would have eluded the searches at LEP and the Tevatron Run 1 in production mechanisms that rely upon the h_fVV coupling. Therefore it is of interest to consider other production mechanisms for h_f which may allow observable rates if the h_fVV coupling is suppressed. Since the couplings h_fVV and h_fVH (where H is another Higgs boson in the model) are complementary, two LEP collaborations, i.e. OPAL [7] and DELPHI [8], also searched for fermiophobic Higgs bosons in the channel $e^+e^- \to A^0h_f$, and ruled out the region $m_A + m_{h_f} < 160$ GeV/c^2. However, a very light $m_{h_f} < 50$ GeV/c^2 is still possible if m_A is sufficiently heavy.

An alternative production mechanism that also depends on the complementary h_fVH coupling is

[1] An angle that diagonalizes the CP-even Higgs matrix.

the process $qq' \to V^* \to h_f H^\pm$. Such a mechanism is exclusive to hadron colliders, and can offer promising rates in Run 2 of the Tevatron provided that $m_{H^\pm}$ in not too far above its present mass bound of $m_{H^\pm} > 90$ GeV/c^2 [16, 17, 18]. In fermiophobic models the decay $H^\pm \to h_f W^{(*)}$ can have a larger BR than the conventional decays $H^\pm \to tb, \tau\nu$. This would lead to double h_f production.

In this study we perform a search for the inclusive production of multi-photon (3 or 4) final states through the mechanism:

$$p\bar{p} \to h_f H^\pm \to h_f h_f W^\pm \to \gamma\gamma\gamma(\gamma) + X. \tag{1}$$

In the Two Higgs Doublet Model (2HDM) the multi-photon signature arises in the parameter space $m_{h_f} < 90$ GeVc^2, $m_{H^\pm} < 200$ GeVc^2, and $\tan\beta > 1$. In this region, BR($h_f \to \gamma\gamma$) ≈ 1 and BR($H^\pm \to h_f W^\pm$)$\approx$1, leading to a 4γ + leptons or jets signature. The multi-photon signature has the added virtue of very small background rates, in contrast to the conventional searches for single h_f production in the channels $\gamma\gamma + V$ and $\gamma\gamma + X$. In [18] it was shown that the multi-photon signal can be observed in a large fraction of the $m_{h_f} \times m_{H^\pm}$ plane at the Tevatron Run 2. In fact, at 95% C.L. Run 2 will be able to exclude Higgs masses up to $m_{H^\pm} < 270$ GeVc^2 for very light m_{h_f}, or $m_{h_f} < 100$ GeV/c^2 for $m_H^\pm \approx 100$ GeVc^2.

2 Signal

For the generation of the signal process we used leading order generation from the PYTHIA [19] event generator. We use $q_i\bar{q}_j \to H^\pm h$ higgs pair-production process with a cascade higgs decay $H^\pm \to W^\pm h$ and a subsequent hadronic decay mode of the W-boson[2]. Together with CTEQ6L1 [20] parton distribution functions, PYTHIA is used for simulation of the rest of the events. Full detector simulation was produced for mass points of: $m_h = 30$ GeV/c^2 and $m_h = 50$ GeV/c^2, with $m_H = 150$ GeV/c^2. For other mass points that were not processed with the full detector simulation, including those with $m_{H^\pm} = 100$ GeV/c^2, we use generator level output (MadGraph II[21]) to extrapolate the acceptance.

3 Data Analysis

3.1 Particle Identification

Photons and electrons are identified in two steps: the selection of the electromagnetic (EM) clusters, and then subsequent separation into those caused by photons or electrons. EM clusters are selected from calorimeter clusters by requiring that (i): at least 97% of the energy be deposited in the EM section of the calorimeter, (ii): the calorimeter isolation[3] to be less than 0.07, (iii): the transverse

[2]We use hadronic mode to calculate the overall signal acceptance. This choice introduces underestimation of signal selection efficiency (due to lower photon-id rate in the presence of jets), and thus results in more conservative results.

[3]Isolation is defined as $[E_{tot}(0.4) - E_{EM}(0.2)]/E_{EM}(0.2)$, where $E_{tot}(0.4)$ is the total shower energy in a cone of radius $R = \sqrt{(\Delta\eta)^2 + (\Delta\phi)^2} = 0.4$, and $E_{EM}(0.2)$ is the EM energy in a cone $R = 0.2$

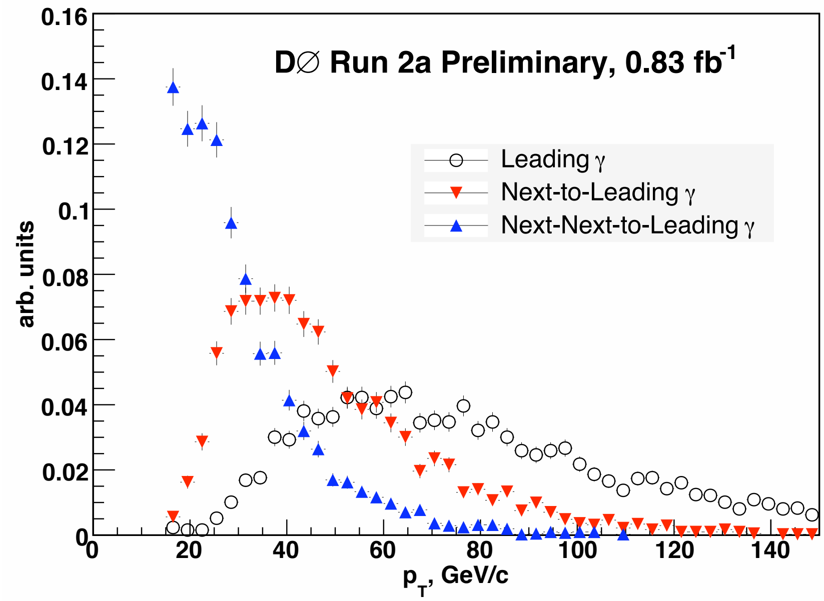

Figure 1: *Spectrum of p_T-ordered photons in signal MC for characteristic signal point: $m_f = 50$ GeV/c^2, $m_{H^\pm} = 150$ GeV/c^2. Distributions are normalized to the total number of events.*

shower profile to be consistent with those expected for an EM shower, and (iv) the scalar p_T sum for all tracks originating from the primary vertex in an annulus of $0.05 < R < 0.4$ around the cluster be less than 2 GeV. The cluster is then defined as an electron if there is a reconstructed track associated with it and a photon otherwise. Jets are reconstructed using the iterative, midpoint cone algorithm [22] with a cone size of $R = 0.5$.

3.2 Tri-photon Data Sample

We select events with three or more photons in the central calorimeter ($|\eta| < 1.1$) with E_T-ordered cuts on their transverse energies: $E_T^{1,2,3} > 30,\ 20,$ and 15 GeV/c^2 (see Fig. 1). Any additional photon, if found, is required to have $E_T > 15$ GeV. Events are required to have primary vertex with $|z_{vtx}| < 60$ cm from the geometrical center of the detector.

3.3 Backgrounds

There are two major sources of the background events. The first comes from the events in which jets or electrons were misidentified as photons. Major sources of these backgrounds are $Z(\rightarrow ee)\gamma$, $W(\rightarrow e\nu)\gamma\gamma$, $3j$, $2j\gamma$, and $j2\gamma$. The other source comes from Direct Triphoton Production (DTP), i.e. Direct Diphoton Production along with the FSR/ISR photon. The contribution of fake events arising from detector noise is estimated to be negligible.

3.3.1 Backgrounds With Misidentified Photons

The estimation of the contribution of events from $Z\gamma$ production is done from a sample of $\{e,e,\gamma\}$ events. We observe 131 such events. The contribution from this process is obtained by weighting the observed number of events with the probability for an electron to be misidentified as a photon ($f_{e\to\gamma} = 0.014 \pm 0.001$): $n^{3\gamma}_{Z\gamma} = N_{Z\gamma} \cdot f^2_{e\to\gamma} = 0.026$ events.

The identification of other backgrounds that contain a $W^\pm$ boson is more involved because they do not have a resonant production on which to make a selection. Therefore, we use the following selection: the contribution of processes with a $W^\pm$ is estimated from $\{e,\gamma,\gamma\}$ events, after the $Z\gamma$ contribution has been subtracted.

We observe 7 events with two photons and one electron. We expect some of them to come from $Z\gamma$ with one lost track: $n^{e\gamma\gamma}_{Z\gamma} = N_{Z\gamma} \cdot 2 \cdot f_{e\to\gamma} = 3.7$ events. An upper limit estimate of the number of events with a $W^\pm$ boson and two photons (real or fake) is $7 - 3.7 = 3.3$ events. Thus, their contribution is also small and comparable to $n^{3\gamma}_{Z\gamma}$: $n^{3\gamma}_{W\gamma\gamma} = 3.3 \cdot 0.014 = 0.046$ events. The overall contribution from processes with W or Z is therefore:

$$n^{3\gamma}_{W/Z+X} = 0.072 \pm 0.036 \text{ events.} \tag{2}$$

QCD backgrounds to the $3\gamma + X$ final state come from direct (fragmentation) photons and/or EM-like jets (denoted by j). They come from the four possible combinations of jets and photons: $\{j,j,j\}$, $\{j,j,\gamma\}$, $\{j,\gamma,\gamma\}$, and $\{\gamma,\gamma,\gamma\}$. The last component can, in principle, contain the Higgs signal. The number of 3γ events that were produced can be obtained by solving four linear equations: $\vec{\mathbf{n}} = \hat{\mathbf{E}} \cdot \vec{\mathbf{N}}$, where $\vec{\mathbf{n}} = (n_{ppp},\ n_{fpp},\ n_{ffp},\ n_{fff})$ denotes a vector of observed events (p=pass, f = fail[4] photon selection) and $\vec{\mathbf{N}} = (N_{\gamma\gamma\gamma},\ N_{j\gamma\gamma},\ N_{jj\gamma},\ N_{jjj})$ denotes produced events. And $\hat{\mathbf{E}}$ is a 4×4 efficiency matrix:

$$\begin{pmatrix} \varepsilon_s^3 & \varepsilon_s^2\varepsilon_b & \varepsilon_s\varepsilon_b^2 & \varepsilon_b^3 \\ 3(1-\varepsilon_s)\varepsilon_s^2 & \varepsilon_s^2(1-\varepsilon_b)+2(1-\varepsilon_s)\varepsilon_s\varepsilon_b & \varepsilon_b^2(1-\varepsilon_s)+2(1-\varepsilon_b)\varepsilon_b\varepsilon_s & 3(1-\varepsilon_b)\varepsilon_b^2 \\ 3(1-\varepsilon_s)^2\varepsilon_s & \varepsilon_b(1-\varepsilon_s)^2+2(1-\varepsilon_s)(1-\varepsilon_b)\varepsilon_s & \varepsilon_s(1-\varepsilon_b)^2+2(1-\varepsilon_b)(1-\varepsilon_s)\varepsilon_b & 3(1-\varepsilon_b)^2\varepsilon_b \\ (1-\varepsilon_s)^3 & (1-\varepsilon_s)^2(1-\varepsilon_b) & (1-\varepsilon_s)(1-\varepsilon_b)^2 & (1-\varepsilon_b)^3 \end{pmatrix} \tag{3}$$

Here the signal and background efficiencies are the probability of a photon and a jet to pass photon-id cuts. The corresponding numerical values are $\varepsilon_s \equiv \varepsilon_\gamma = 0.75 \pm 0.05$ and $\varepsilon_b \equiv f_{j\to\gamma} = 0.043 \pm 0.004$. These numbers can be understood as effective photon efficiency and jet fake rate in this background sample. Slight difference in the p_T spectrum between $\{j,j,j\}$, $\{\gamma,j,j\}$, and $\{\gamma,\gamma,j\}$ samples results in additional 3% uncertainty.

The following numbers of events observed are: $\vec{\mathbf{n}} = (5,\ 27,\ 169,\ 246)$. The solution of four linear equations gives us the number of events that were produced in the collisions: $\vec{\mathbf{N}} = (10.1,\ 19.1,\ 175,\ 233)$. Thus, the QCD contribution from $\{j,j,j\}$, $\{j,j,\gamma\}$, and $\{j,\gamma,\gamma\}$ processes is estimated to be:

[4] To remove electrons from W's and Z's, physics objects that fail photon cuts are required not to have associated track.

$$n^{3\gamma}_{QCD} = 0.72 \pm 0.15 \text{ events.} \tag{4}$$

Thus, the total background that comes from events with at least on misidentified photon is estimated to be

$$n^{3\gamma}_{fake} = 0.8 \pm 0.15 \text{ events.} \tag{5}$$

3.3.2 Direct Tri-Photon Background

We estimate the DTP background in the following way. We scale the corrected number of di-photon events observed in data ($N^{\gamma\gamma}(Data)$) with the rate at which one would expect to observe a third photon in Direct-Diphoton-Production (DDP) processes from PYTHIA:

$$N^{3\gamma}_{DTP} = \frac{N_{\gamma\gamma\gamma}(MC)}{N\gamma\gamma(MC)} \cdot N^{\gamma\gamma}(Data) \cdot \rho. \tag{6}$$

Here, because the di-photon data sample contains a non-negligible fraction of $\gamma + j$ and $j + j$ events, we apply a purity factor, $\rho = n^{2\gamma}_{DDP}/(n^{2\gamma}_{DDP} + n^{2\gamma}_{\gamma+j} + n^{2\gamma}_{j+j})$.

We extract ρ from data using a matrix method similar to the one employed in the previous section. This time, however, we compose a 3×3 efficiency matrix and relate contributions from $\{\gamma,\gamma\}$, $\{\gamma, j\}$, and $\{j, j\}$ processes to the $n_{i,j}$ numbers of observed two-body events. Here, indices i and j can be p or f, and as before, $p(f)$ indicates – "passed(failed) the photon-id cuts". The number of observed events that pass/fail photon cuts is given by the following expression: $\vec{\mathbf{n}} = (n_{pp},\ n_{pf},\ n_{ff}) = (3.5 \cdot 10^3,\ 37.3 \cdot 10^3,\ 108.1 \cdot 10^3)$.

The contributions of $W/Z + X$ to $\{\gamma,\gamma\}$ are found to be negligible in comparison with the total di-photon count, and thus we proceed with solving for the number of produced events: $\vec{\mathbf{N}} = \{N_{\gamma\gamma}, N_{j\gamma}, N_{jj}\} = \{3.7 \cdot 10^3,\ 37.4 \cdot 10^3,\ 107.8 \cdot 10^3\}$. This gives individual contributions to he observed diphoton final state: $\{n^{2\gamma}_{\gamma+j},\ n^{2\gamma}_{j+j},\ n^{2\gamma}_{DDP}\} = \{1.2 \cdot 10^3,\ 0.2 \cdot 10^3,\ 2.1 \cdot 10^3\}$, resulting in purity: $\rho = n^{2\gamma}_{DDP}/(n^{2\gamma}_{DDP} + n^{2\gamma}_{\gamma+j} + n^{2\gamma}_{j+j}) = 0.61 \pm 0.12$.

Now, we can proceed with the estimation of DTP. From PYTHIA MC of DDP events, the fraction of DTM is found to be $n^{3\gamma}_{DTP}/n^{total}_{DDP} = (1.3 \pm 0.4) \cdot 10^{-3}$ and gives the estimated DTP background as:

$$n^{3\gamma}_{DTP} = 2.73 \pm 0.55 \text{ events.} \tag{7}$$

3.3.3 Total Background

The total background to the $3\gamma + X$ final state is estimated to be the sum of $n^{3\gamma}_{DTP} = 2.73 \pm 0.55$ and $n^{3\gamma}_{fake} = 0.80 \pm 0.15$: $n_{bkg} = 3.5 \pm 0.6$ events. Figure 2 shows the distribution of the di-photon invariant mass in data and from the expected backgrounds. Note that each event contributes three histogram entries (three possible photon-photon combinations), *e.g.* for data there are 15 entries, although we observe 5 events. The overall agreement is good and we can see that the data follow the general shape of the background.

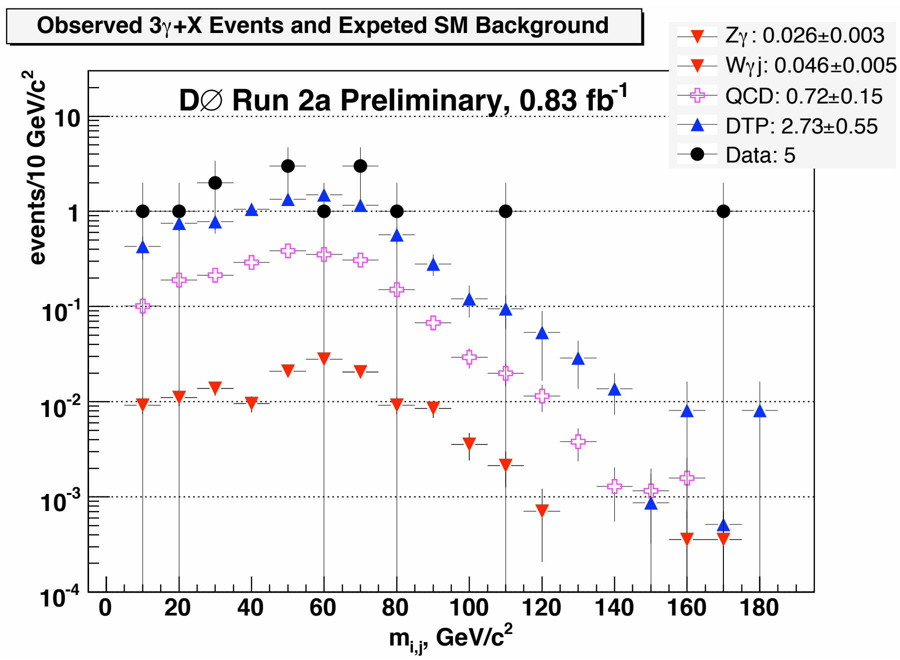

Figure 2: *Distribution of two-body invariant mass for $3\gamma+X$ events observed in data and expected SM background. Note that each event contributes three entries – $m_{1,2}$, $m_{1,3}$, and $m_{2,3}$. One event which contributes entries $m_{2,3} = 54.2$ GeV/c^2 and $m_{1,3} = 165$ GeV/c^2 also has an entry which is not shown – $m_{1,2} = 236$ GeV/c^2.*

4 Signal-Background discriminant

Let us recall that the underlying signal event has four photons and two jets or a lepton from a W. Each object is quite energetic carrying on average 10-20 GeV/c of momentum in the transverse plane. Thus a system of only three photons recoiling against the rest of the event would be rather imbalanced in p_T, with the recoil particle(s) carrying away the rest of the collision energy. Background events, on the other hand are expected to be balanced in p_T. The total transfer momentum of a 3-body system can be written as

$$H_T \equiv \sqrt{\left(\sum_{i=1}^{3} p_x^i\right)^2 + \left(\sum_{i=1}^{3} p_y^i\right)^2}. \tag{8}$$

where the sum goes over the 3 objects passing photon selection and all other event requirements. Any 4-particle background event with one of the particles failing the selection cuts will have H_T similar to that found in signal events. However, such background should be suppressed by a factor proportional to the rate of 4-jet events in the 3-jet sample which is proportional to $\approx 10^{-3} - 10^{-2}$.

Figure 3 shows the distribution of the transverse momentum of the 3-body system, photons for signal MC, and objects that fail photon selection in data. From the optimization of $\varepsilon_s^{H_T}/\sqrt{\varepsilon_s^{H_T} + \varepsilon_b^{H_T}}$ we obtain an optimal cut value of $H_T^{cut} = 25$ GeV/c. The corresponding efficiencies for the H_T requirement are: $\varepsilon_{H_T>25}^{\text{signal}} = 0.92 \pm 0.01$ and $\varepsilon_{H_T>25}^{\text{bkg}} = 0.30 \pm 0.01$. After this cut the expected background is reduced to 1.1 events with zero events passing this cut in data:

$$n_{SM\ exp.}^{3\gamma+X} = 1.1 \pm 0.2, \tag{9}$$

$$n_{Data\ obs.}^{3\gamma+X} = 0. \tag{10}$$

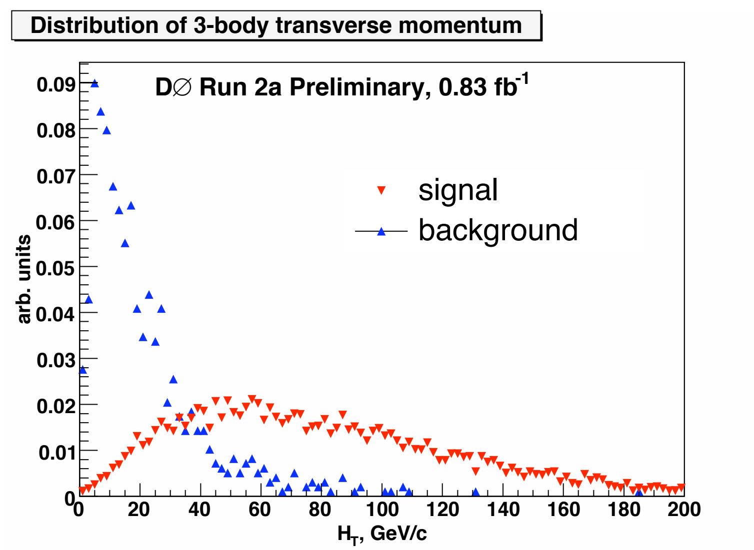

Figure 3: *Distribution of H_T of 3 most energetic central photons in signal MC and in $3j$ background in data sample. A cut $H_T > 25$ GeV/c is found to be 92% efficient for the signal while reducing the background by 70%.*

5 Limit

In the absence of excess of events in data we proceed with setting an upper limit [23, 24] on the Higgs boson production cross section allowed by this analysis at the 95% confidence level:

$$\sigma_{CL_s}^{95\%} = 25.3 \text{ fb}. \tag{11}$$

	value	uncertainty
Number or observed events	0	–
Number of expected background events	1.1	0.20
Integrated Luminosity	0.83 fb^{-1}	0.05
Signal Acceptance	0.16	0.03

Table 1: *Summary of quantities used in the calculation of the upper cross-section limit.*

Limits are calculated using Bayesian statistics with a flat prior probability for the signal cross section. Quantities used for calculation of this limit are summarized in Table 1. All errors are treated as 100% uncorrelated.

Figure 4 shows the production cross section for several benchmark points overlaid with the obtained upper limit. A region to the left of the mass at which the exclusion curve intersects the theoretical production cross section corresponds to the excluded mass region of the fermiophobic Higgs. The benchmark exclusion is as follows:

- $m^{95\%}_{C.L._{h_f}} \geq 66$ GeV/c^2 for $m_{H^\pm} \leq 100$ GeV/c^2, $\tan\beta = 3$;
- $m^{95\%}_{C.L._{h_f}} \geq 44$ GeV/c^2 for $m_{H^\pm} \leq 150$ GeV/c^2, $\tan\beta = 3$;
- $m^{95\%}_{C.L._{h_f}} \geq 80$ GeV/c^2 for $m_{H^\pm} \leq 100$ GeV/c^2, $\tan\beta = 30$;
- $m^{95\%}_{C.L._{h_f}} \geq 50$ GeV/c^2 for $m_{H^\pm} \leq 150$ GeV/c^2, $\tan\beta = 30$.

The results shown in Fig. 4 represent the first excluded region for a fermiophobic Higgs boson in the class of Two Higgs Doublets Models.

References

[1] H. E. Haber, G. L. Kane, and T. Sterling, Nucl. Phys. **B161**, 493 (1979); J. F. Gunion, R. Vega, and J. Wudka, Phys. Rev. D **42**, 1673 (1990); J. L. Basdevant, E. L. Berger, D. Dicus, C. Kao, and S. Willenbrock, Phys. Lett. B **313**, 40(1993); V. Barger, N. G. Deshpande, J. L. Hewett, and T. G. Rizzo, separate Higgs, Report No. OITS-499, hep-ph/9211234; P. Bamert and Z. Kunszt, Phys. Lett. B **306**, 335 (1993); A. G. Akeroyd, 368, 89 (1996) ; M. C. Gonzalez-Garcia, S. M. Lietti, and S. F. Novaes, Phys. Rev. D **57**, 7045 (1998); A. Barroso, L. Brucher, and R. Santos, Phys. Rev. D **60**, 035005 (1999); L. Brucher and R. Santos, Eur. Phys. J. C 12, **87** (2000).

[2] B. Dobrescu, Phys. Rev. D (to be published), Report No. FERMILAB-PUB-99/234-T, hep-ph/9908391; B. Dobrescu, G.Landsberg, and K. Matchev, FERMILAB-PUB-99/324-T.

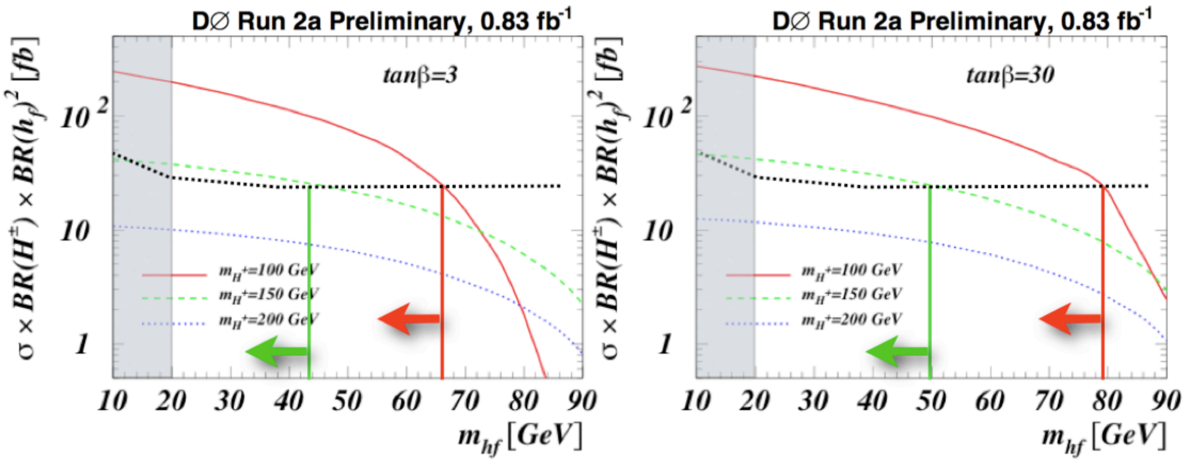

Figure 4: *Exclusion regions for four benchmark points. Results obtained from the 95% CL cross-section limit (black dotted line) on the* $\sigma(q\bar{q} \to H^{\pm}h \to 3\gamma + X)$ *processes. Regions to the left of the vertical lines correspond to the excluded Higgs masses, e.g.* $m^{95\%}_{C.L.} = 80$ GeV/c^2 *for* $m_{H^\pm} \leq 100$ GeV/c^2, $\tan\beta = 30$.

[3] L. Hall and C. Kolda, Phys. Lett. B **459**, 213 (1999); H. Cheng, B. A. Dobrescu, and C. T. Hill, Electroweak symmetry breaking and extra dimensions, Report No. FERMILAB-PUB-99/358-T, hep-ph/9912343.

[4] M. Carena, S. Mrenna, and C. E. Wagner, Phys. Rev. D **60**, 075010 (1999).

[5] S. Mrenna, talk given at PASCOS99, Lake Tahoe, California, 1999.

[6] A. Djouadi, M. Spira, and P. M. Zerwas, Phys. Lett. B **311**, 255 (1993); A. Stange, W. Marciano, and S. Willenbrock, Phys. Rev. D **49**, 1354 (1994); M. A. Diaz and T. J. Weiler, Decays of a fermiophobic Higgs, Report No. VAND-TH-94-1, hep-ph/9401259; K. Melnikov, M. Spira, and O. Yakovlev, Z. Phys. C **64**, 401 (1994) ; S. Moretti and W. J. Stirling, Phys. Lett. B 347, 291 (1995); Y. Liao and X. Li, 396, 225 (1997); M. Steinhauser, "Corrections to the decay of an intermediate-mass Higgs boson into two photons", Report No. MPI-PHT-96-130, hep-ph/9612395; A. Djouadi, "Decays of the Higgs bosons", Report No. PM-97-51, hep-ph/9712334.

[7] G. Abbiendi *et al.* [OPAL Collaboration], Phys. Lett. B **544**, 44 (2002).

[8] P. Abreu *et al.* [DELPHI Collaboration], Phys. Lett. B **507**, 89 (2001); Eur. Phys. J. C **35**, 313, (2004).

[9] A .Heister *et al.* [ALEPH Collaboration], Phys. Lett. B **544**, 16 (2002).

[10] P. Achard *et al.* [L3 Collaboration], Phys. Lett. B **534**, 28 (2002); Phys. Lett. B **568**, 191 (2003).

[11] B. Abbott et al. [DØ Collaboration], Phys. Rev. Lett. **82**, 2244 (1999).

[12] T. Affolder et al. [CDF Collaboration], Phys. Rev. D **64**, 092002 (2001).

[13] V. M. Abazov et al. [D0 Collaboration], arXiv:hep-ex/0508054.

[14] G. Landsberg and K. T. Matchev, Phys. Rev. D **62**, 035004 (2000).

[15] A. Melnitchouk [D0 Collaboration], Int. J. Mod. Phys. A **20**, 3305 (2005).

[16] A. G. Akeroyd and M. A. Diaz, Phys. Rev. D **67**, 095007 (2003).

[17] A. G. Akeroyd, M. A. Diaz and F. J. Pacheco, Phys. Rev. D **70**, 075002 (2004).

[18] A. G. Akeroyd, A. Alves, M. A. Diaz and O. Eboli, arXiv:heph/0512077 (2005).

[19] Sjoestrand, T. et al., PYTHIA 6.3 Physics and Manual, hep-ph/0308153 (2003).

[20] CTEQ6 Parton Distributions, hep-ph/0512167 (2005).

[21] F. Maltoni, Madevent: Automatic Event Generation with MADGRAPH, hep-ph/0208156 (2002).

[22] G. C. Blazey et al., in Proceedings of the Workshop: "QCD and Weak Boson Physics in Run II" edited by U. Baur, R. K. Ellis, and D. Zeppenfeld, 47 (2000). See Section 3.5 for details.

[23] J. Hobbs et al., Numerical Bayesian Limit Calculator.

[24] R.T. Cox, Am. J. Phys. **14**, 1 (1946); H. Jeffreys, "*Theory of Probability*", 3rd edition, Oxford University Press (1961); E.T. Jaynes and L. Bretthorst, "*Probability Theory, the Logic of Science*", Oxford, 2003; A. O'Hagan, "*Kendall's Advanced Theory of Statistics, Volume 2B: Bayesian Inference*", Oxford (1994).